International Journal of Heat and Mass Transfer 70 (2014) 119–127

Contents lists available at ScienceDirect

International Journal of Heat and Mass Transfer

journal homepage: www.elsevier.com/locate/ijhmt

Natural convection in an enclosure containing a sinusoidally heated cylindrical source

R. Roslan [a], H. Saleh [b], I. Hashim [b,c,*], A.S. Bataineh [d]

[a] Faculty of Science, Technology & Human Development, Universiti Tun Hussein Onn Malaysia, 86400 Parit Raja, Johor, Malaysia
[b] School of Mathematical Sciences, Universiti Kebangsaan Malaysia, 43600 UKM Bangi, Selangor, Malaysia
[c] Solar Energy Research Institute, Universiti Kebangsaan Malaysia, 43600 UKM Bangi, Selangor, Malaysia
[d] Department of Mathematics, Faculty of Science, Al Balqa Applied University, 19117 Salt, Jordan

ARTICLE INFO

Article history:
Received 22 November 2012
Received in revised form 18 September 2013
Accepted 5 October 2013

Keywords:
Natural convection
Square enclosure
Inner cylinder

ABSTRACT

The problem of unsteady natural convection induced by a temperature difference between a cold outer square enclosure and a hot inner circular cylinder is studied in this paper. The cylinder temperature is assumed to vary sinusoidally with time about a fixed mean temperature. The coupled momentum and energy equations have been solved numerically over a wide range of values of the amplitude and the frequency of the source temperature signal, as well as the source radius. It is found that the heat transfer rate tends to increase by oscillating the source temperature signal. The maximum heat transfer augmentation was obtained for frequency between 25π and 30π for a high amplitude and a moderate source radius.

1. Introduction

Fluid flow and natural heat transfer from a heated body, especially cylinder inside enclosures has long been studied and has received much attention due to its direct relevancy to many engineering applications such as flooding protection for buried pipes, solidification processes, heat exchangers, electronic packaging and chemical reactors. House et al. [1] investigated the effect of a centered, conducting body and concluded that heat transfer process across the enclosure may be increased or decreased by a conducting body with a thermal conductivity ratio lower or greater than unity, respectively. Ghaddar [2] studied a uniformly heated horizontal cylinder placed in a large air-filled rectangular enclosure and found the maximum air velocity was at a distance of about nine cylinder diameters along the vertical centerline above the heated cylinder. Moukalled and Acharya [3] and Shu and Zhu [4] analyzed the effect of the radius of the inner cylinder and the aspect ratio to the fluid flow and heat transfer rate. Cesini et al. [5] performed a numerical and experimental analysis of a horizontal cylinder and reported in general the numerical and experimental result were in good accordance. Shu et al. [6] employed the differential quadrature method and showed that the global circulation, flow separation and the top space between the square outer enclosure and circular inner cylinder have an important influence on the flow and thermal fields. A heated cylinder kept in a square enclosure with different thermal boundary conditions was presented by Roychowdhury et al. [7].

Angeli et al. [8] developed a correlation for the average Nusselt number as a function on both the Rayleigh number and the cylinder diameter. The heat transfer enhancement by increasing the cylinder size and/or surface emissivity was obtained by Mezrhab et al. [9]. Kim et al. [10] and Lee et al. [11] showed that the cylinder position could affect heat transfer quantities. The changes in heat transfer quantities at Rayleigh number of 10^7 was presented by Yoon et al. [12] and Yu et al. [13]. Hussain and Hussein [14] studied a uniform heat source applied on the inner cylinder in a square air filled enclosure in which all boundaries are assumed to be isothermal. They obtained a two-cellular flow field and found that the total average Nusselt number behaves nonlinearly as a function of locations. The existence of local peaks of the Nusselt number along the surfaces of the cylinder and the enclosure was investigated by Lee et al. [11]. Recently, Nabavizadeh et al. [15] studied a heated sinusoidal cylinder at various amplitudes and undulations. They concluded that increasing amplitude or number of undulations or changing the angle might change the heat transfer coefficient which then influence the temperature and velocity fields. Very recently, Sairamu and Chhabra [16] considered a heated tilted square cylinder placed at the center of a square enclosure.

The transient behavior of fluid flow and heat transfer in an enclosure has been extensively studied due to the relevance to many industrial applications. For example, in the cooling of electronic

* Corresponding author at: School of Mathematical Sciences, Universiti Kebangsaan Malaysia, 43600 UKM Bangi, Selangor, Malaysia. Tel.: +60 3 8921 5758; fax: +60 3 8925 4519.
E-mail address: ishak_h@ukm.my (I. Hashim).

0017-9310/$ - see front matter © 2013 Elsevier Ltd. All rights reserved.
http://dx.doi.org/10.1016/j.ijheatmasstransfer.2013.10.011

Nomenclature

a, A	amplitude, dimensionless amplitude
F	dimensionless oscillating frequency
g	gravitational accleration
n	normal direction to the walls
ℓ	width and height of enclosure
p, P	pressure, dimensionless pressure
Nu	Nusselt number
Pr	Prandtl number
r, R	cylinder radius, dimensionless cylinder radius
Ra	Rayleigh number
t	time
T	temperature
$\overline{T}_h$	mean value of hot temperature
u, v	velocity components in the x- and y-directions
U, V	dimensionless velocity components in the X- and Y-directions
W	surface area of walls
x, y & X, Y	space coordinates & dimensionless space coordinates

Greek symbols

α	thermal diffusivity
β	thermal expansion coefficient
ν	kinematic viscosity
θ	angle of circular cylinder
Θ	dimensionless temperature
τ	dimensionless time
$\ddot{\tau}$	dimensionless time at stable state
τ_p	dimensionless periodic time of cylinder temperature
ρ	density
ω	oscillating frequency
$\overline{Nu}_{ss}$	average Nusselt number at basic steady state
$\overline{Nu}$	time-averaged Nusselt number

subscripts

c	cold
h	hot
ss	steady

equipment, the electrical components are periodically energized intermittently and, therefore, the heating is an unsteady manner. Kazmierczak and Chinoda [17] investigated natural convection of water in a square enclosure by sinusoidal heating. Antohe and Lage [18] reported the convection intensity within the enclosure increases linearly with heating amplitude, while the resonance frequency was shown to be independent of the heating amplitude. Abourida et al. [19] and El Ayachi et al. [20] indicated that the heat transfer in a system could be enhanced by a proper choice of the considered parameters. Cheikh et al. [21] concluded that the periodical heating case causes an increase of the mean heat transfer in comparison to the constant heating case. Liu et al. [22] studied a square conducting body placed at the center of the enclosure. It was found that the resonant frequency decreases by increasing the body size and thermal conductivity ratio. In the problem of chaotic natural convection, Al-Taey [23] found the appearance of a new chaotic form in the stream function pattern and temperature distribution when he studied a heated square enclosure with time periodic boundary conditions. Recently, Zhang et al. [24] proposed the high-accuracy solutions of the sinusoidal heating profile. The aim of the present work is to investigate numerically the problem of unsteady natural convection from a sinusoidally heated cylinder embedded in a square enclosure. The sinusoidal heating is predicted to contribute the heat transfer enhancement due to the pulsating local flow response around the cylinder, for example the periodically on/off circular light in a room would enhance the heat transfer mechanism across the room.

2. Mathematical formulation

A schematic diagram of a cold square enclosure having an inner hot circular cylinder is shown in Fig. 1(a). The cylinder with radius r is located in the center of the enclosure and its temperature varies sinusoidally in time about a mean hot temperature $\overline{T}_h$, with amplitude a and frequency ω. The cylinder or source temperature is hotter than the wall temperature at all times, as graphically depicted in Fig. 1(b). Under the influence of the vertical gravitational field, the cylinder and walls at different levels of temperature lead to a natural convection problem. The fluid is assumed Newtonian and viscous dissipation and radiation effects are negligible. We assumed the cylinder and walls were made from materials having very low emissivity such as the polished aluminium, so that radiation has a very small effect on the temperature of the cylinder and walls. The governing equations are described by the NavierStokes and the energy equations, respectively. The governing equations are transformed into dimensionless forms under the following non-dimensional variables

$$\tau=\frac{t\alpha}{\ell^2},\quad X=\frac{x}{\ell},\quad Y=\frac{y}{\ell},\quad U=\frac{u\ell}{\alpha},\quad V=\frac{v\ell}{\alpha},\quad \Theta=\frac{T-T_c}{\overline{T}_h-T_c},$$
$$R=\frac{r}{\ell},\quad Pr=\frac{\nu}{\alpha},\quad Ra=\frac{g\beta(\overline{T}_h-T_c)\ell^3}{\nu\alpha},\quad P=\frac{p\ell^2}{\rho\alpha},\quad A=\frac{a}{\overline{T}_h-T_c},$$
$$F=\frac{\omega\ell^2}{\alpha}. \tag{1}$$

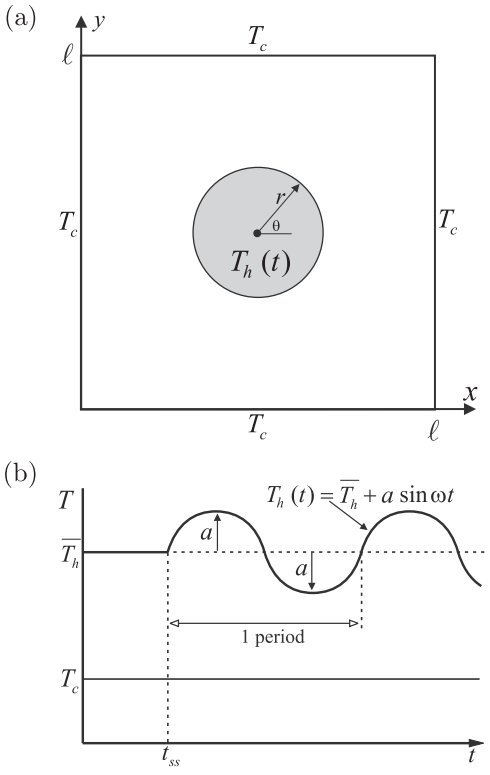

Fig. 1. Schematic representation of the model.

Table 1
Grid sensitivity checks at $Ra = 10^5$ and $R = 0.2$ in a steady state.

Predefined mesh size	Mesh elements	$\overline{Nu}_{ss}$	CPU time (s)
Extremely coarse	254	4.6638	4
Extra coarse	472	4.9806	4
Coarser	648	5.0448	5
Coarse	1076	5.3533	5
Normal	1584	5.3717	6
Fine	2444	5.3480	7
Finer	7626	5.1354	15
Extra fine	21420	5.1039	39
Extremely fine	26828	5.0845	49

The dimensionless forms of the governing equations are expressed in the following forms:

$$\frac{\partial U}{\partial X} + \frac{\partial V}{\partial Y} = 0, \tag{2}$$

$$\frac{\partial U}{\partial \tau} + U\frac{\partial U}{\partial X} + V\frac{\partial U}{\partial Y} = -\frac{\partial P}{\partial X} + Pr\left(\frac{\partial^2 U}{\partial X^2} + \frac{\partial^2 U}{\partial Y^2}\right), \tag{3}$$

$$\frac{\partial V}{\partial \tau} + U\frac{\partial V}{\partial X} + V\frac{\partial V}{\partial Y} = -\frac{\partial P}{\partial Y} + Pr\left(\frac{\partial^2 V}{\partial X^2} + \frac{\partial^2 V}{\partial Y^2}\right) + RaPr\Theta, \tag{4}$$

Table 2
Comparison of the present $\overline{\overline{Nu}}$ results with literatures for the case of a differentially heated vertical enclosure and $R = 0$, $Ra = 1.4 \times 10^5$ and $Pr = 7$.

A	F	Present work	[21]	[17]
0.4	100	5.45	5.43	5.41
0.8	100	5.63	5.61	5.58
0.4	200	5.41	5.38	5.36

$$\frac{\partial \Theta}{\partial \tau} + U\frac{\partial \Theta}{\partial X} + V\frac{\partial \Theta}{\partial Y} = \left(\frac{\partial^2 \Theta}{\partial X^2} + \frac{\partial^2 \Theta}{\partial Y^2}\right), \tag{5}$$

where $U = V = 0$ on the walls and cylinder. The initial and boundary conditions for the non-dimensional temperatures are:

$\Theta = 0$, at $\tau = 0$
$\Theta = 0$, on walls
$\Theta = 1 + A\sin(F\tau)$, on cylinder surface

The rate of heat transfer is computed at inner wall expressed in terms of the local surface Nusselt number (Nu) as:

$$Nu = \frac{\partial \Theta}{\partial \xi} \tag{6}$$

where ξ is the angular location. The surface-averaged Nusselt number ($\overline{Nu}$) on the hot circular wall is evaluated as

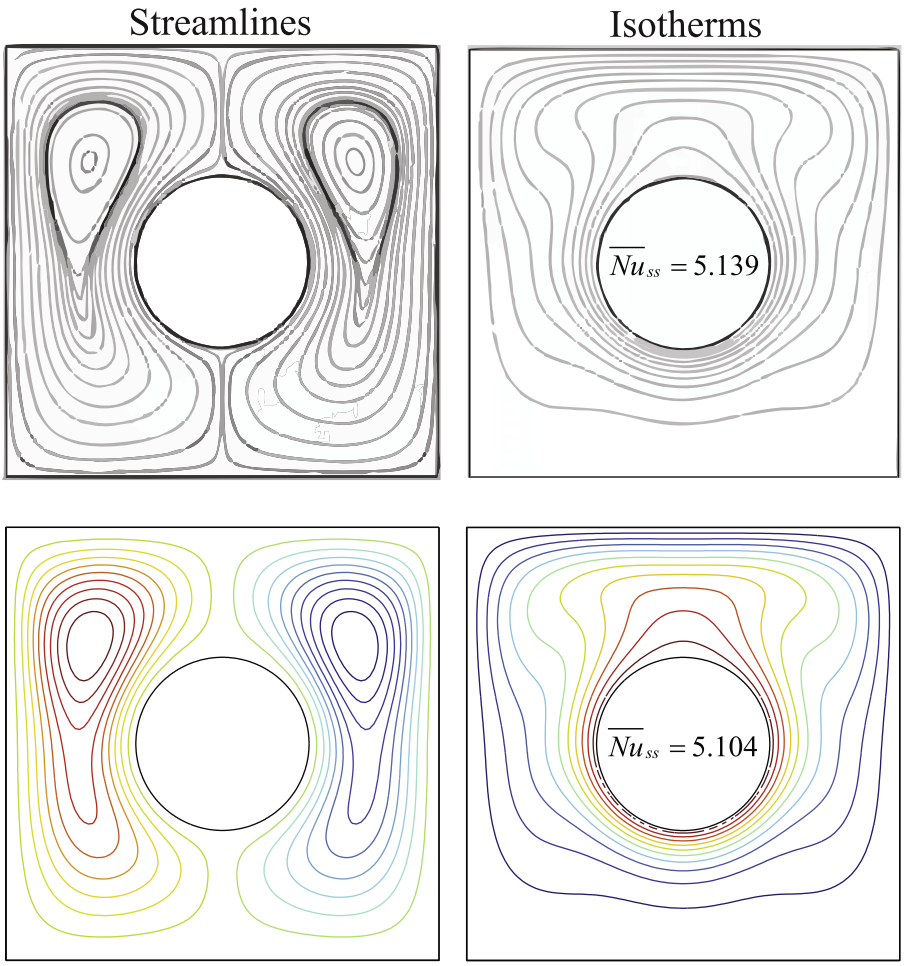

Fig. 2. Comparison of computed streamlines and isotherms present work (bottom) with Kim et al. [10] (top) results in a steady state at $Ra = 10^5$ and $R = 0.2$.

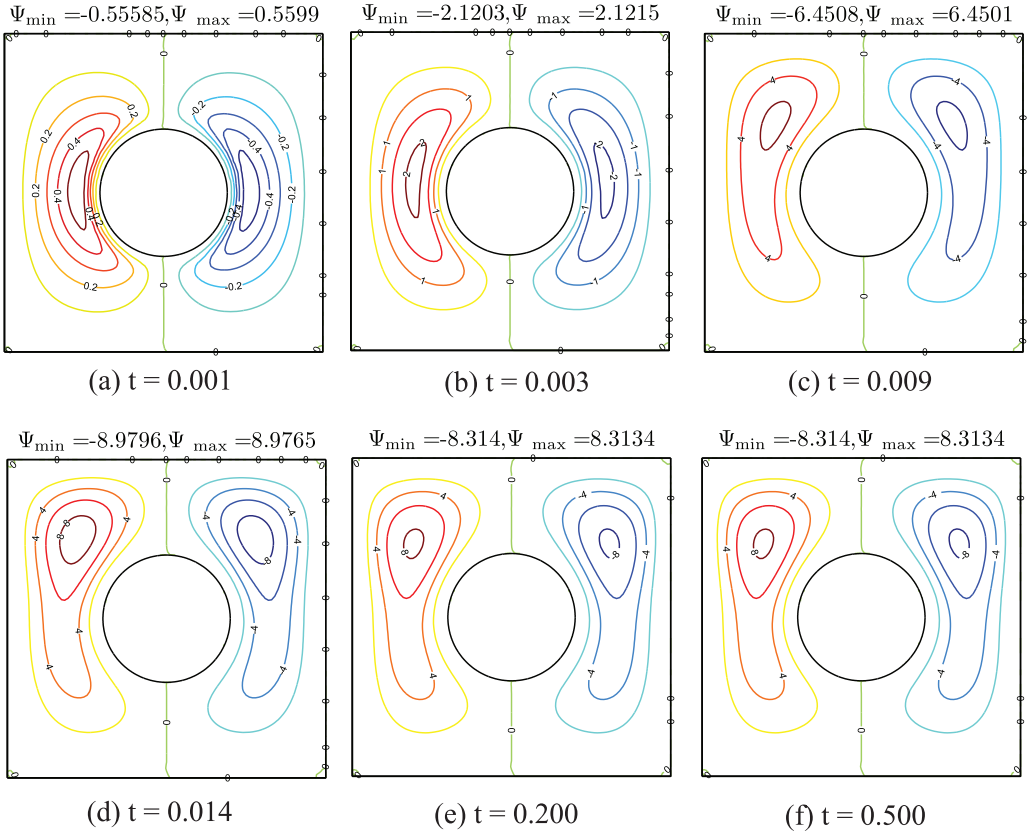

Fig. 3. Time history of streamlines at $R = 0.2$ and $Ra = 10^5$.

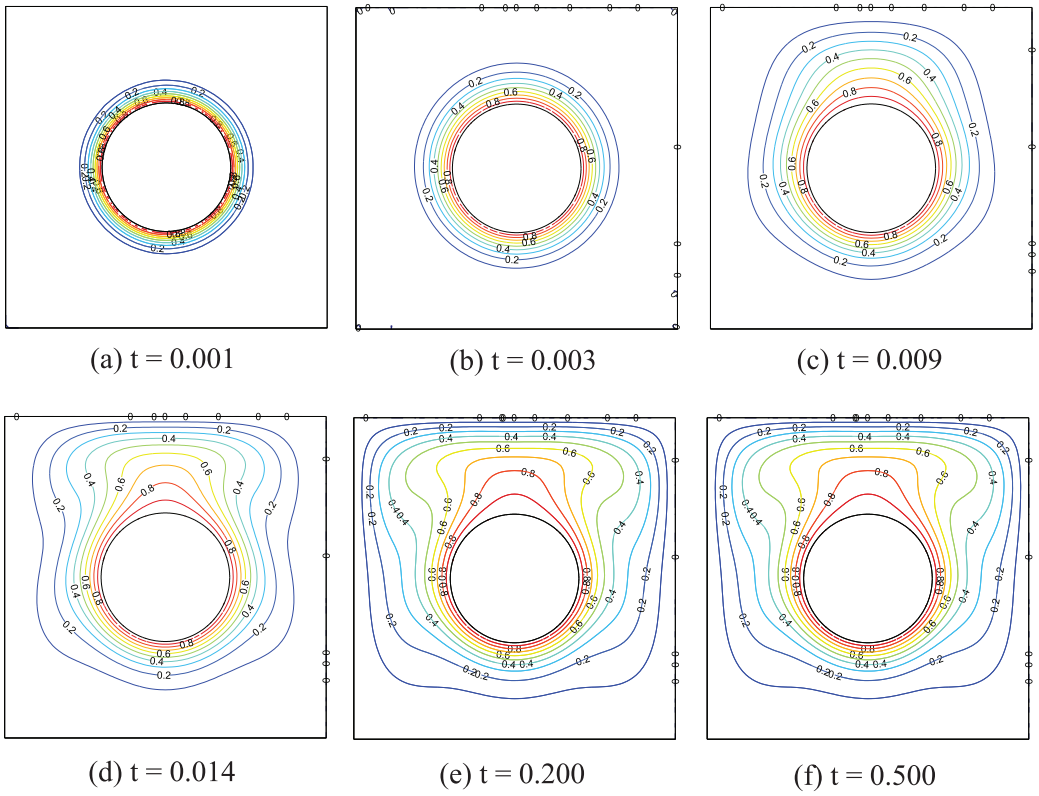

Fig. 4. Time history of temperature fields at $R = 0.2$ and $Ra = 10^5$.

$$Nu = \frac{1}{2\pi}\int_0^{360^\circ} Nu(\xi)\mathrm{d}\xi \tag{7}$$

3. Computational methodology

The governing equations along with the boundary conditions are modelled and solved numerically by COMSOL, a general-purpose solver of interlinked partial differential equation (PDE) based on the Galerkin finite element method (GFEM). This software contains state-of-the-art numerical algorithms and visualization tools bundled together with an easy to use interface. We consider the following application modes in COMSOL: The incompressible, laminar flow (spf) for Eqs. (2)–(4) and the heat transfer in fluids (ht) for Eq. (5). P2-P1 Lagrange elements and the Galerkin least-square method are used to assure stability.

In this study, mesh generation on square enclosure with cylinder is made by using triangles. Several grid sensitivity tests were conducted to determine the sufficiency of the mesh scheme and to ensure that the results are grid independent. We use the COMSOL default settings for predefined mesh sizes, i.e. extremely coarse, extra coarse, coarser, coarse, normal, fine, finer, extra fine and extremely fine. In the tests, we consider the parameters $Ra = 10^5$ and $R = 0.2$ in a steady state as tabulated in Table 1. Considering both accuracy and time, a finer mesh size was selected for all the computations done in this paper. As a validation, our results for the streamline and isotherms compare well with those obtained by Kim et al. [10] for a steady case at $Ra = 10^5$ and $R = 0.2$ as shown in Fig. 2. An additional verification of accuracy for the present code is shown in Table 2 for the unsteady condition and the case of a differentially heated vertical enclosure with $Ra = 1.4 \times 10^5$ and $Pr = 7$. We observe that the comparison was in good agreement with the results reported in the literatures [17,21].

4. Results and discussion

The analysis in the undergoing numerical investigations is performed in the following domain of the associated dimensionless

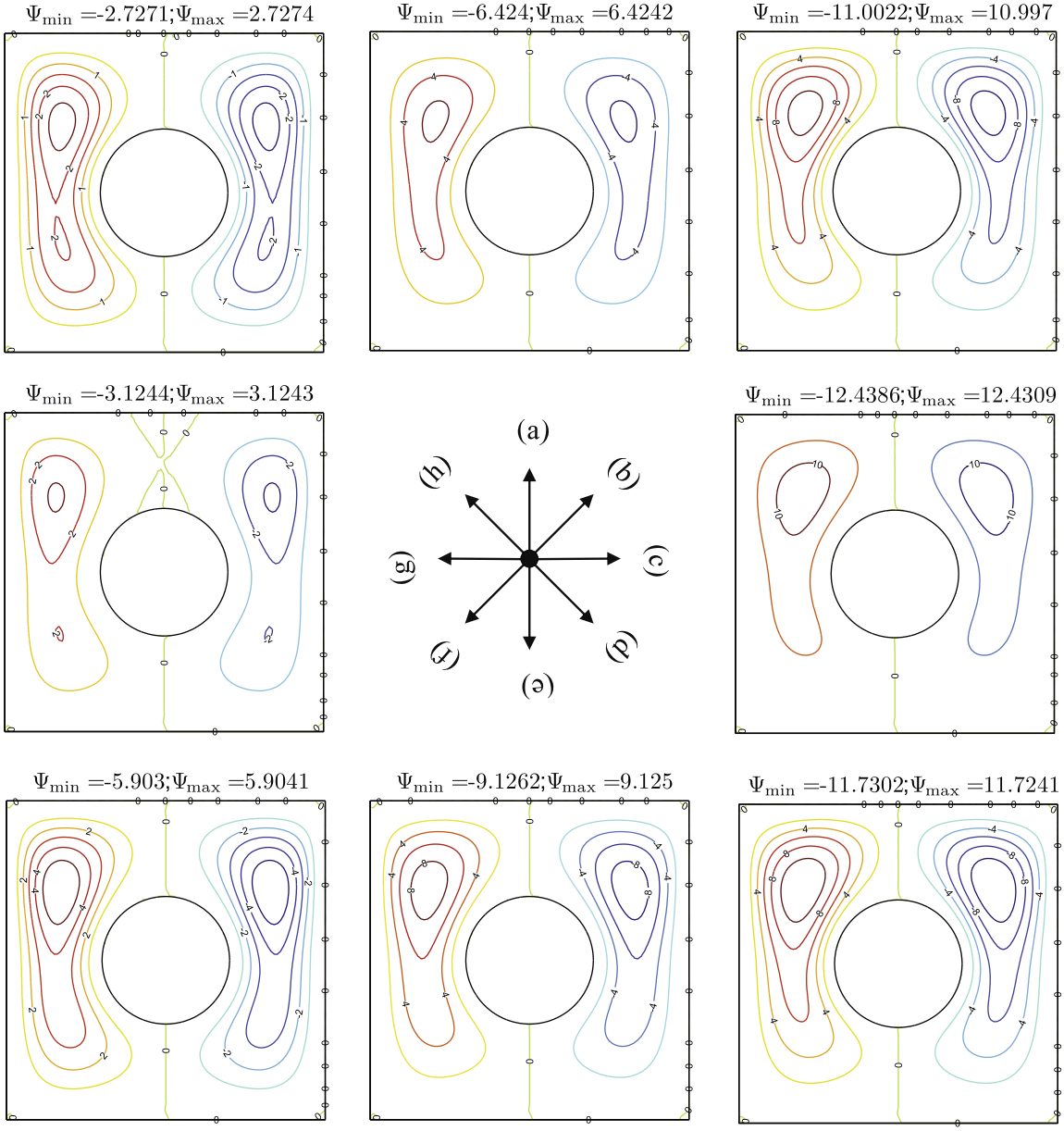

Fig. 5. Sequential contour plots of flow fields during one period for $R = 0.2$, $Ra = 10^5$, $A = 0.8$ and $F = 20\pi$ when (a) $\tau = \ddot{\tau}$, (b) $\tau = \ddot{\tau} + \tau_p/8$, (c) $\tau = \ddot{\tau} + 2\tau_p/8$, (d) $\tau = \ddot{\tau} + 3\tau_p/8$, (e) $\tau = \ddot{\tau} + 4\tau_p/8$, (f) $\tau = \ddot{\tau} + 5\tau_p/8$, (g) $\tau = \ddot{\tau} + 6\tau_p/8$ and (h) $\tau = \ddot{\tau} + 7\tau_p/8$.

groups: the Rayleigh number, $10^3 \leqslant Ra \leqslant 10^6$, the heating amplitude, $0.1 \leqslant A \leqslant 0.9$, the oscillating frequency, $5\pi \leqslant F \leqslant 50\pi$, and the cylinder radius, $0.05 \leqslant R \leqslant 0.3$. The Prandtl number is fixed at $Pr = 0.7$.

4.1. Effect of the time dependency on flow and temperature fields

Figs. 3 and 4 show the transient results of the flow and temperature fields for the non-oscillating case at $R = 0.2$ and $Ra = 10^5$, respectively. Initially, at $\tau = 0$, the cylinder and walls are cold and there is no fluid motion in the region between the cylinder and walls. At the very beginning after the start of heating ($0.001 < \tau < 0.003$), the fluid temperature adjoining the hot cylinder rises, and the buoyancy force promotes an upward flow at the sides of the cylinder. This movement creates an anti-clockwise circulation cell in the left-half enclosure and clockwise circulation cell in the right-half enclosure. The isotherms are circular-parallel to the circumference line of the cylinder. This implies that conduction or diffusion mode is dominant. For $\tau = 0.009$, it is observed that the core of the both cell starts to move upward and the strength of the flow circulation increases significantly. The isotherms start to bend. This implies that the onset of convection has occurred. As time increases, the temperature has been well distributed from the hot cylinder to the top cold wall, so that the anti-clockwise and clockwise flows are intensified in the top portion of the enclosure. Insignificant differences of flow and temperature fields are observed when time takes longer, at $\tau = 0.5$. This implies the steady state has been reached at the previous time, at $\tau = 0.2$.

After the basic steady state has been reached, the next phase is to investigate the effect of the temperature oscillation. Figs. 5 and 6 show the evolutions of the flow and temperature fields in one period or cycle. We fix the heating amplitude $A = 0.8$, oscillating frequency $F = 20\pi$, cylinder radius $R = 0.2$ and $Ra = 10^5$. In order to obtain a stable state, $\ddot{\tau}$, three oscillating cycles were calculated. The subplots (a)–(h) correspond to the eight phases from $\tau = \ddot{\tau}$ to $\tau = \ddot{\tau} + 7\tau_p/8$ in the fourth cycle. We note that the results of the fifth cycle are identical to the results of the fourth cycle. At the beginning, the streamline shows that two symmetrical flow circu-

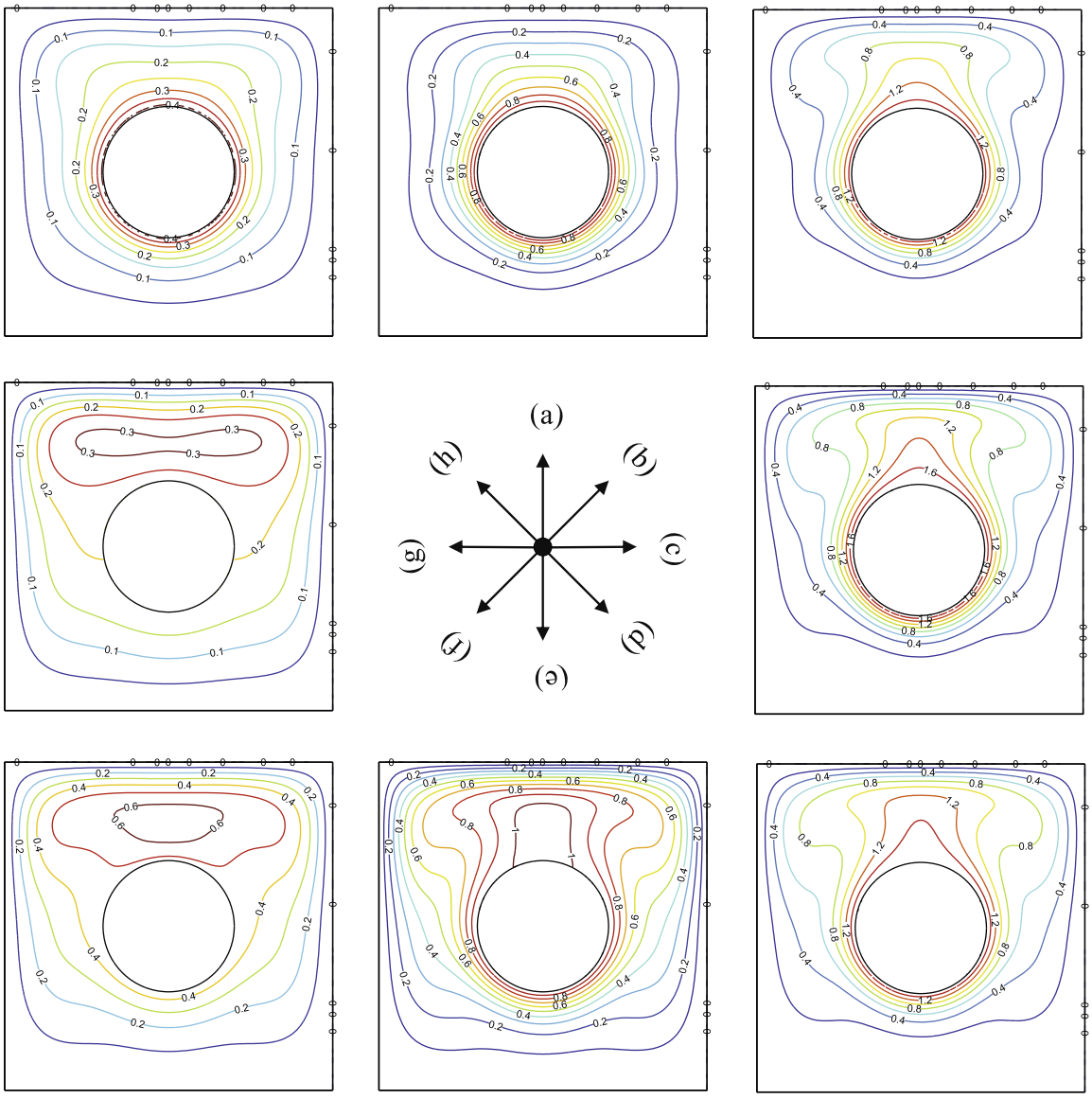

Fig. 6. Sequential contour plots of temperature fields during one period for $R = 0.2$, $Ra = 10^5$, $A = 0.8$ and $F = 20\pi$ when (a) $\tau = \ddot{\tau}$, (b) $\tau = \ddot{\tau} + \tau_p/8$, (c) $\tau = \ddot{\tau} + 2\tau_p/8$, (d) $\tau = \ddot{\tau} + 3\tau_p/8$, (e) $\tau = \ddot{\tau} + 4\tau_p/8$, (f) $\tau = \ddot{\tau} + 5\tau_p/8$, (g) $\tau = \ddot{\tau} + 6\tau_p/8$ and (h) $\tau = \ddot{\tau} + 7\tau_p/8$.

lations exist with the inner vortices located in the upper half of the enclosure. As time increases, both flows are intensified and a plume starts to appear on the top of the cylinder as shown in the isotherms. The plume is strengthened by increasing time further, which also leads to the formation of a thinner thermal boundary layer near the top wall. The warm-chamber appears at $\tau = \ddot{\tau} + 5\tau_p/8$, the time at which the cylinder temperature is less than the mean temperature. The warm-chamber is a room above the top of the cylinder having a fairly high temperature. The warm-chamber is elongated horizontally and less warmer than before at $\tau = \ddot{\tau} + 6\tau_p/8$. At this time, two inner vortices appear in the streamlines. The two inner vortices grow in size at $\tau = \ddot{\tau} + 7\tau_p/8$, but the strength of the two symmetrical flow circulations decreases and reaches its minimum value.

4.2. Parameter effects on heat transfer rate

Fig. 7 shows temporal evolution of the $\overline{Nu}$ for various values of A at $R = 0.2$, $Ra = 10^5$ and $F = 20\pi$. The heat transfer rate oscillates with periodic variation of the source temperature signal for all amplitudes considered in this study. Perfectly sinusoidal laws were found for all A values. The cylinder temperature oscillation with large amplitude causes a substantial amplification of flow, therefore, the instantaneous of the flow differs much from the non-oscillating case. These affects yield wider fluctuating of $\overline{Nu}$ when A takes higher. Moreover, the instantaneous values of $\overline{Nu}$ reaches negative values for case $A = 0.9$

Fig. 8 shows temporal evolution of the $\overline{Nu}$ for various values of F at $R = 0.2$, $Ra = 10^5$ and $A = 0.8$. Perfectly sinusoidal laws were

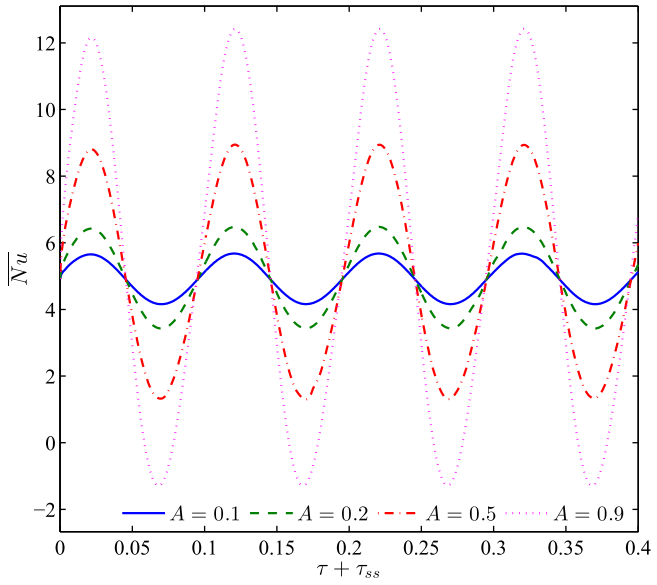

Fig. 7. Time–dependent behavior of $\overline{Nu}$ for various values of A at $R = 0.2$, $Ra = 10^5$ and $F = 20\pi$.

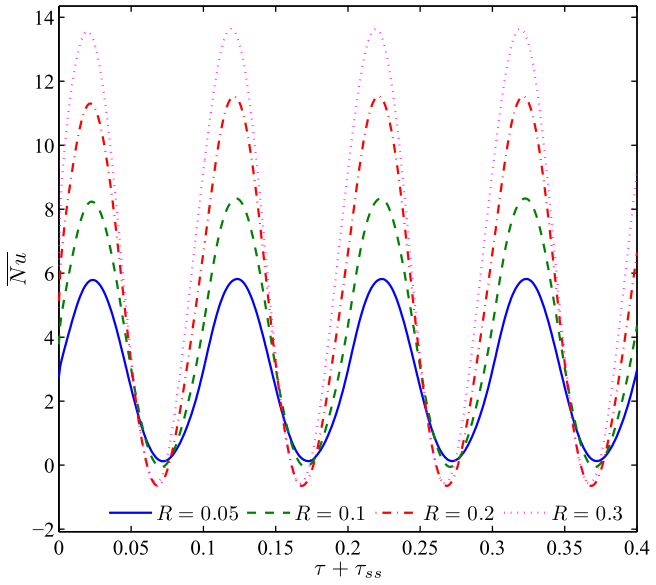

Fig. 9. Time–dependent behavior of $\overline{Nu}$ for various values of R at $F = 20\pi$ and $A = 0.8$, $Ra = 10^5$.

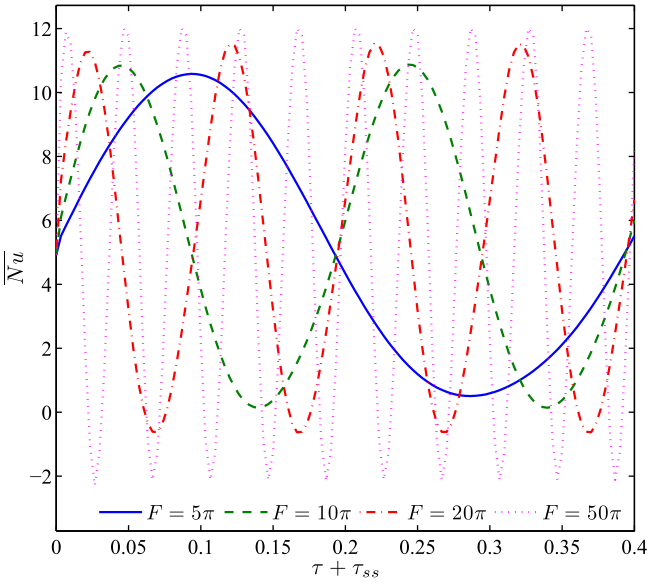

Fig. 8. Time–dependent behavior of $\overline{Nu}$ for various values of F at $R = 0.2$, $Ra = 10^5$ and $A = 0.8$.

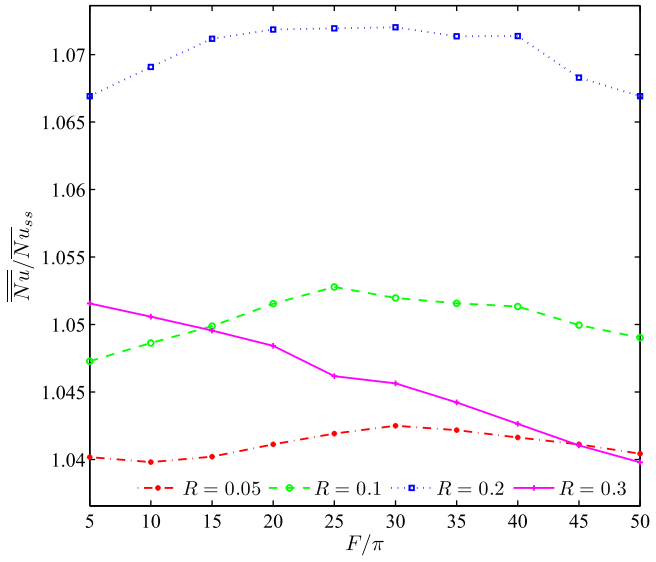

Fig. 10. The normalized $\overline{Nu}$ against frequency for various values of R at $A = 0.8$ and $Ra = 10^5$.

found for all oscillating frequencies. The fluctuating amplitude of $\overline{Nu}$ increases slightly as F increases. This is due to the fact that at a high frequency, the duration for hot temperature distribution is much shorter. The results in Fig. 8 indicate the presence of a phase-leg among the wall-temperature signal and the instantaneous $\overline{Nu}$. The phase-leg changes with frequency since frequency modifies fluid particle velocity.

Fig. 9 shows temporal evolution of the $\overline{Nu}$ for various values of R at $F = 20\pi$ and $A = 0.8$, $Ra = 10^5$. Perfectly sinusoidal laws were found for all values of cylinder radius studied. The maximum value of the temporal $\overline{Nu}$ over each period increases significantly by increasing the source radius. However, the minimum value of the temporal $\overline{Nu}$ over each period was almost unchanged by varying the source radius. It is also observed that the locations of the minimum and maximum values vary with R. From Figs. 7–9, we can conclude that the fluctuating amplitude of $\overline{Nu}$ increases as A, F or R increases. Or alternatively, the fluctuating amplitude shrinks to zero as A, F or R goes to zero. This indicates that there is no periodic flow or heat transfer oscillation in the system. We observe that there exists a critical value of A, F or R for the onset of periodic flow. Currently, our numerical scheme cannot detect accurately the critical value of A, F or R, but roughly from Figs. 7–9 the critical values are in the range $0 < A < 0.1$, $0 < F < 5\pi$ and $0 < R < 0.05$.

The time-averaged Nusselt number, $\overline{\overline{Nu}}$ over the average Nusselt number at basic state, $\overline{Nu}_{ss}$ with the oscillating frequency, F, for $R = 0.05, 0.1, 0.2$ and 0.3 at $A = 0.8$ and $Ra = 10^5$ is presented in Fig. 10. The oscillating frequency is limited in the range 5π to 50π. It was observed that for all R, the ratio $\overline{\overline{Nu}}/\overline{Nu}_{ss}$ is always more than 1. This indicates heat transfer augmentation for the considered R and F range. The case $R = 0.2$ has the best heat transfer augmentation for the considered F interval. From Fig. 10, we can see the normalized Nusselt number reaches a maximum value roughly at frequency 25π to 30π for $R \leqslant 0.2$.

Fig. 11 presents the ratio $\overline{\overline{Nu}}/\overline{Nu}_{ss}$ with the frequency of the source temperature signal for various heating amplitudes at $R = 0.2$. Larger A results in bigger augmentation of $\overline{\overline{Nu}}$. At low heating amplitudes, the heat transfer performance is constant by increasing the frequency. It is also observed that there is almost no heat transfer augmentation for these amplitudes. This phenomenon is due to the fact that the fluid does not fell the presence of

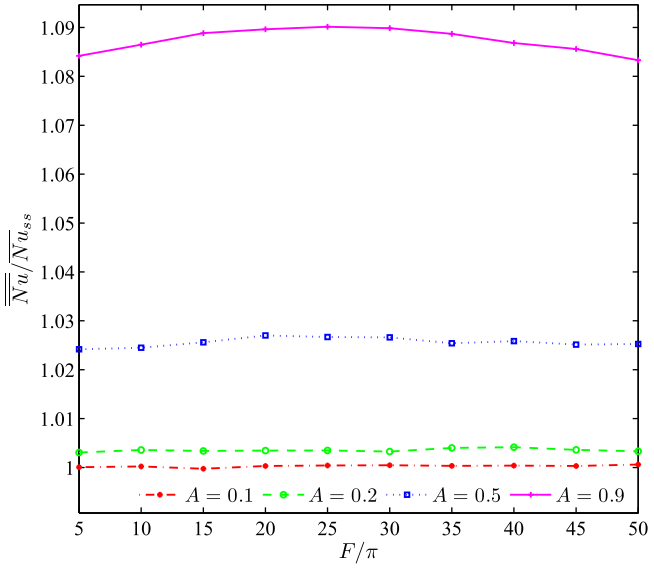

Fig. 11. The normalized $\overline{Nu}$ against frequency for various values of A at $R = 0.2$ and $Ra = 10^5$.

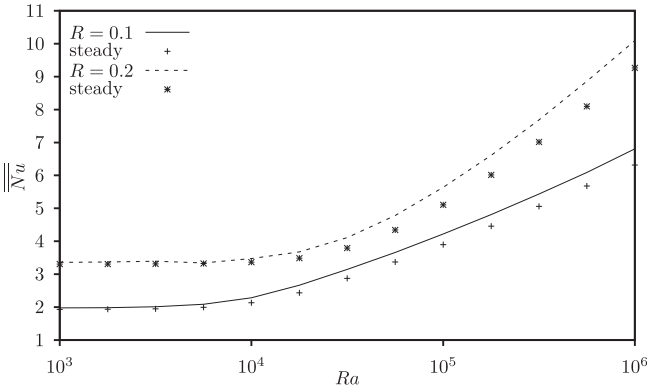

Fig. 12. The $\overline{\overline{Nu}}$ against Rayleigh number for various values of R at $A = 0.8$ and $F = 20\pi$.

the hot source temperature oscillation, thus the deviation of the time-averaged $\overline{\overline{Nu}}$ from the basic state $\overline{Nu}$ is small. The normalized Nusselt number reaches a maximum value at about $F = 25\pi$ for high heating amplitudes. Note specifically that the $\overline{\overline{Nu}}/\overline{Nu}_{ss}$ decreases continuously when increasing the frequency for cylinder radius of 0.3. A bigger cylinder means a larger hot surface that brings a stronger buoyancy force, but it also leads to a smaller space for the fluid to circulate that restrains the fluid movement. That way, initially oscillating the surface temperature at very low frequency penetrates and stimulates the fluid velocities near the surface that increases the thermal performance of the system, but the system can not response properly to the temperature oscillation for further increasing the frequency at the narrow fluid space. It tends to decrease the overall thermal performance or reduce the $\overline{\overline{Nu}}/\overline{Nu}_{ss}$. But $\overline{\overline{Nu}}$ is still above the $\overline{Nu}_{ss}$.

Fig. 12 presents the time-averaged Nusselt number against Rayleigh number for $R = 0.1, 0.2$ at $A = 0.8$ and $F = 20\pi$. We also integrated the Nusselt number for the basic steady for the corresponding R. The Nusselt number increases by increasing the Rayleigh number for the considered R. Also, the Nusselt number increases by increasing the cylinder radius for the fixed Ra. Fig. 12 also shows that initially at relative low Ra, no heat transfer augmentation was found by oscillating the surface temperature. At moderate Ra, oscillating the surface temperature enhances the Nusselt number slightly compared to the corresponding steady values. Later, increasing Ra yields a stronger heat transfer augmentation. Finally, the time-averaged Nusselt number can be correlated pretty well with R and Ra as follows:

$$\overline{\overline{Nu}} = \left(7^{\frac{R}{0.104}} + 0.033\,Ra\right)^{0.183+\frac{R}{2}}. \tag{8}$$

This correlation is valid for $10^3 \leqslant Ra \leqslant 10^6$ and $0.075 \leqslant R \leqslant 0.225$. Note that the maximum error is less than 5% for the valid ranges.

5. Conclusions

The present numerical simulations study deal with buoyancy-driven flows in an isothermal square enclosure where a heat cylindrical heat source is centred. The dimensionless forms of the governing equations are modeled and solved by using the COMSOL package. Detailed computational results for flow and temperature fields and the heat transfer have been presented in graphical forms. The main conclusions of the present analysis are as follows:

1. The cylinder temperature oscillation can drastically change the flow and temperature fields. Two inner vortices were found in the flow field and a warm-chamber existed in the temperature field due to the effect of heated cylinder temperature oscillation.

2. The periodic heat transfer rate perfectly followed a sinusoidal law for the considered parameters. Its maximum value of the temporal increases significantly by increasing the cylinder radius, but its minimum value was almost unchanged by varying the cylinder radius.
3. Heat transfer rate tends to increase by oscillating the source temperature signal. The maximum heat transfer augmentation was obtained at about frequency 25π to 30π for a high heating amplitude and a moderate source radius.

Acknowledgments

The authors would like to thank the reviewers for the comments which led to an improvement in the paper. This work was supported by the Universiti Kebangsaan Malaysia's Grant No. DIP-2012-12.

References

[1] J. House, C. Beckermann, T. Smith, Effect of a centered conducting body on natural convection heat transfer in an enclosure, Numer. Heat Transfer Part A 18 (1990) 213–225.
[2] N.K. Ghaddar, Natural convection heat transfer between a uniformly heated cylindrical element and its rectangular enclosure, Int. J. Heat Mass Transfer 35 (1992) 2327–2334.
[3] F. Moukalled, S. Acharya, Natural convection in the annulus between concentric horizontal circular and square cylinders, J. Thermophys. Heat Transfer 10 (1996) 524–531.
[4] C. Shu, Y.D. Zhu, Efficient computation of natural convection in a concentric annulus between an outer square cylinder and an inner circular cylinder, Int. J. Numer. Methods Fluid 38 (2002) 429–445.
[5] G. Cesini, M. Paroncini, G. Cortella, M. Manzan, Natural convection from a horizontal cylinder in a rectangular cavity, Int. J. Heat Mass Transfer 42 (1999) 1801–1811.
[6] C. Shu, H. Xue, Y.D. Zhu, Numerical study of natural convection in an eccentric annulus between a square outer cylinder and a circular inner cylinder using DQ method, Int. J. Heat Mass Transfer 44 (2001) 3321–3333.
[7] D. Roychowdhury, S. Das, T. Sundararajan, Numerical simulation of natural convective heat transfer and fluid flow around a heated cylinder inside an enclosure, Heat Mass Transfer 38 (2002) 565–576.
[8] D. Angeli, P. Levoni, G.S. Barozzi, Numerical predictions for stable buoyant regimes within a square cavity containing a heated horizontal cylinder, Int. J. Heat Mass Transfer 51 (2008) 553–565.
[9] A. Mezrhab, M.A. Moussaoui, H. Naji, Lattice Boltzmann simulation of surface radiation and natural convection in a square cavity with an inner cylinder, J. Phys. D: Appl. Phys. 41 (2008) 115502.
[10] B.S. Kim, D.S. Lee, M.Y. Ha, H.S. Yoon, A numerical study of natural convection in a square enclosure with a circular cylinder at different vertical locations, Int. J. Heat Mass Transfer 51 (2008) 1888–1906.
[11] J.M. Lee, M.Y. Ha, H.S. Yoon, Natural convection in a square enclosure with a circular cylinder at different horizontal and diagonal locations, Int. J. Heat Mass Transfer 53 (2010) 5905–5919.
[12] H.S. Yoon, M.Y. Ha, B.S. Kim, D.H. Yu, Effect of the position of a circular cylinder in a square enclosure on natural convection at Rayleigh number of 10^7, Phys. Fluids 21 (2009) 047101.
[13] D.H. Yu, H.S. Yoon, M.Y. Ha, Numerical study of natural convection in a square enclosure with an inner circular cylinder for Rayleigh number of 10^7, Trans. Korean Soc. Mech. Eng. B 34 (2010) 739–747.
[14] S.H. Hussain, A.K. Hussein, Numerical investigation of natural convection phenomena in a uniformly heated circular cylinder immersed in square enclosure filled with air at different vertical locations, Int. Commun. Heat Mass Transfer 37 (2010) 1115–1126.
[15] S.A. Nabavizadeh, S. Talebi, M. Sefid, M. Nourmohammadzadeh, Natural convection in a square cavity containing a sinusoidal cylinder, Int. J. Therm. Sci. 51 (2012) 112–120.
[16] M. Sairamu, R.P. Chhabra, Natural convection in power-law fluids from a tilted square in an enclosure, Int. J. Heat Mass Transfer 56 (2013) 319–339.
[17] M. Kazmierczak, Z. Chinoda, Buoyancy-driven flow in an enclosure with time periodic boundary conditions, Int. J. Heat Mass Transfer 35 (1992) 1507–1518.
[18] B.V. Antohe, J.L. Lage, Natural convection in an enclosure under time periodic heating: an experimental study, Am. Soc. Mech. Eng. Heat Transfer Div. 324 (1996) 57–64.
[19] B. Abourida, M. Hasnaoui, S. Douamna, Transient natural convection in a square enclosure with horizontal walls submitted to periodic temperatures, Numer. Heat Transfer Part A 36 (1999) 737–750.
[20] R. El Ayachi, A. Raji, M. Hasnaoui, A. Bahlaoui, Combined effect of radiation and natural convection in a square cavity differentially heated with a periodic temperature, Numer. Heat Transfer Part A 53 (2008) 1339–1356.
[21] N.B. Cheikh, B.B. Beya, T. Lili, Aspect ratio effect on natural convection flow in a cavity submitted to a periodical temperature boundary, J. Heat Transfer 129 (2007) 1060–1068.
[22] D. Liu, F.Y. Zhao, G.F. Tang, Conjugate heat transfer in an enclosure with a centered conducting body imposed sinusoidal temperature profiles on one side, Numer. Heat Transfer Part A 53 (2007) 204–223.
[23] K.A. Al-Taey, Natural convection in a laterally and volumetrically heated square enclosure with time-periodic boundary conditions, Int. J. Heat Technol. 27 (2009) 77–85.
[24] W. Zhang, G. Xi, C. Zhang, Z. Huang, A high-accuracy temporal-spatial pseudospectral method for time-periodic unsteady fluid flow and heat transfer problems, Int. J. Comput. Fluid Dyn. 25 (2011) 191–206.